THE ASTROPHYSICAL JOURNAL, 266:298–308, 1983 March 1

THE HYDROGEN-DEPLETED PLANETARY NEBULAE ABELL 30 AND ABELL 78

GEORGE H. JACOBY
Kitt Peak National Observatory

AND

HOLLAND C. FORD[1]
University of California, Los Angeles; and Space Telescope Science Institute
Received 1982 May 12; accepted 1982 August 26

ABSTRACT

Both Abell 30 and Abell 78 exhibit remarkable morphological disparities between their images in [O III] λ5007 and Hα λ6563. This is due to hydrogen depletion in the inner regions of the two planetary nebulae. The material appears to be the end product of a hydrogen-burning shell which has subsequently been ejected. With the exception of helium and possibly carbon, the relative abundances of the other elements are, in general, normal. One of the knots in Abell 30, however, seems to be significantly deficient in oxygen and neon. The helium abundances relative to hydrogen are extremely high, with typical values by number of 6–10; these numbers show that hydrogen has been nearly completely converted to helium. The frequency of occurrence of planetary nebulae having helium-enriched shells of this type is discussed.

Subject headings: nebulae: abundances — nebulae: individual — nebulae: planetary

I. INTRODUCTION

Abell 30 and Abell 78 were first suspected of being unusual by Greenstein and Minkowski (1964), based on spectra of the central stars and the immediately adjacent regions. Emission lines from highly ionized elements were seen (e.g., O VI at 128 eV), and Hα was very weak or absent, suggesting very high temperature, hydrogen-deficient central stars.

Subsequently, Cohen and Barlow (1974) measured the 10 μm fluxes from Abell 30 and Abell 78 and found that they differed significantly from values expected for their nebular densities. Cohen and Barlow and later, Cohen *et al.* (1977) determined that the infrared emission is produced in an extended 10″ radius region centered on their central stars. Jacoby (1979) and Hazard *et al.* (1980) showed that in both nebulae the infrared emission coincides with knots which are bright at [O III] λ5007 and He II λ4686 but undetectable in the hydrogen Balmer lines.

Hazard *et al.* took spectra of one of the central knots in Abell 30 and found that, except for the striking absence of hydrogen lines, the knot is similar to a high-excitation planetary nebula. This led those authors to the inevitable conclusion that the inner knots in Abell 30 have been depleted of their hydrogen content. In this paper, we confirm the findings of Hazard *et al.* and extend the observations to additional knots in Abell 30 and to the inner nebulosity in Abell 78.

[1] Visiting Observer, Kitt Peak National Observatory, which is managed by the Association of Universities for Research in Astronomy, Inc., under contract with the National Science Foundation.

II. OBSERVATIONS AND REDUCTIONS

Because of the nearly simultaneous discovery of the knots in Abell 30 by Jacoby (1979) and Hazard *et al.* (1980), the knots are numbered differently in the two papers. For example, we observed knots 3 and 4 (Jacoby), corresponding to knots 4 and 3 (Hazard)! Aside from any possible prejudices, we choose to use Jacoby's notation because he identified four knots, whereas Hazard *et al.* identified only three. Note that number 1 in Hazard's list is identified as a nearby star.

We made all observations of Abell 30 in 1980 November at the KPNO 4 m telescope using the intensified image dissector scanner (IIDS) with an entrance aperture of 3″.2. We also observed Abell 78 similarly in the red (4700–6800 Å); its blue region of the spectrum (3500–5200 Å) was observed in 1981 October using identical instrumental parameters. Additional data for Abell 78 was obtained at the Lick Observatory 3 m telescope using a comparable instrumental system. Spectral resolution (FWHM) is about 6 Å in the blue, 7 Å in the red, and 11 Å for the Lick data (3500–6000 Å).

We observed Abell 30 in the usual beam-switch mode with each of the instrument's two apertures (separated by 53″) alternately observing the knot. The outer shell of Abell 78 is somewhat brighter than that of Abell 30, requiring the "nebular" mode of observation in which both apertures are first on the extended object and then both are moved off to the sky. Although this results in half as much observing time for the central nebulosity in Abell 78, additional information is gathered on the outer nebulosity. The inner region observed in Abell 78 is midway between the central star and the nearby star 10″ to the northeast.

1983ApJ...266..298J

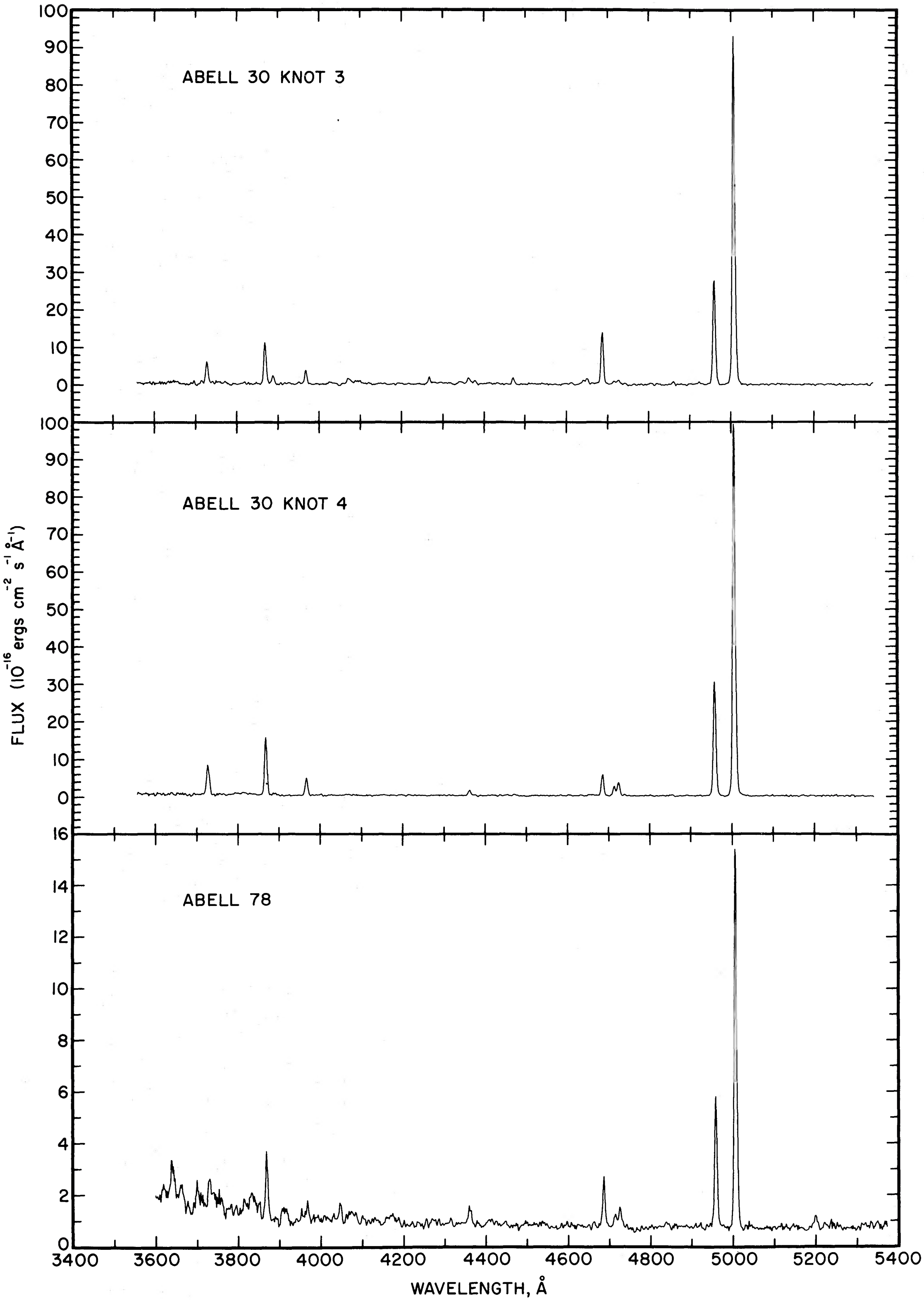

FIG. 1.—The blue spectral region of the hydrogen-depleted shells in the planetary nebulae Abell 30 and Abell 78

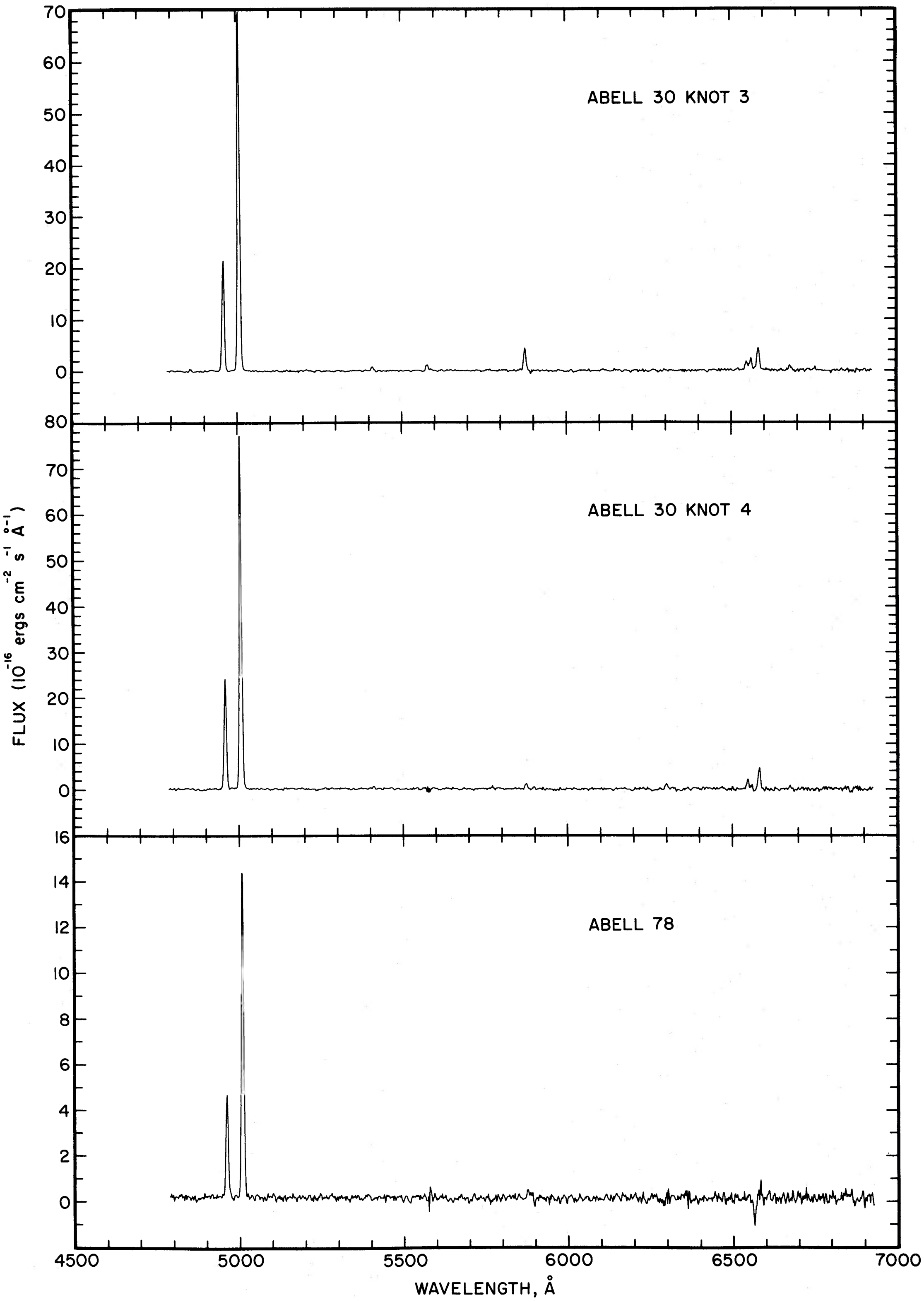

FIG. 2.—The red spectral region of the hydrogen-depleted shells in the planetary nebulae Abell 30 and Abell 78

Figures 1 and 2 show the resulting spectra for Abell 30 knots 3 and 4 and for Abell 78. Figures 3 and 4 show the same spectra as Figures 1 and 2 for Abell 30, but the vertical scale has been magnified to provide better detail of the weaker lines. The data from the outer nebulosity of Abell 78 (not shown here) is noisy but suggests a more normal chemical composition, with Hβ comparable to He II λ4686 in strength. This is consistent with the recent photoelectric photometry results presented by Kaler (1981). Table 1 lists our measurements for the line strengths relative to the intensity of [O III] λ5007. This line, rather than Hβ, was chosen as the reference because it is present in each spectral region observed and has the least uncertainty due to measurement error. The reddening correction is likewise normalized at λ5007 and is derived from Whitford's (1958) reddening curve. The values for $c(\mathrm{H}\beta)$, the logarithmic reddening correction at λ4861, are also given for reference. These values are derived from the visual extinction of the central stars as calculated by Cohen *et al.* (1977).

Because there is dust across the central regions of these planetary nebulae, these extinction values may not be correct for any or all of the nubulosities. This suspicion is reinforced by Kaler's (1981) data which suggest little or no extinction in the line of sight to the outer nebulosities. However, the reddening corrections adopted here are small and have little effect on the subsequent conclusions and are in part justified by the spatial coincidence of the observed nebulosities with the infrared-emitting dust known to be present (Cohen *et al.* 1977; Greenstein 1980).

In Table 1 line ratios are given as averages when multiple observations are available, e.g., $I(\lambda4959)/I(\lambda5007)$. The uncertainties in the Abell 78 line ratios are less than 30% for lines stronger than 10% of

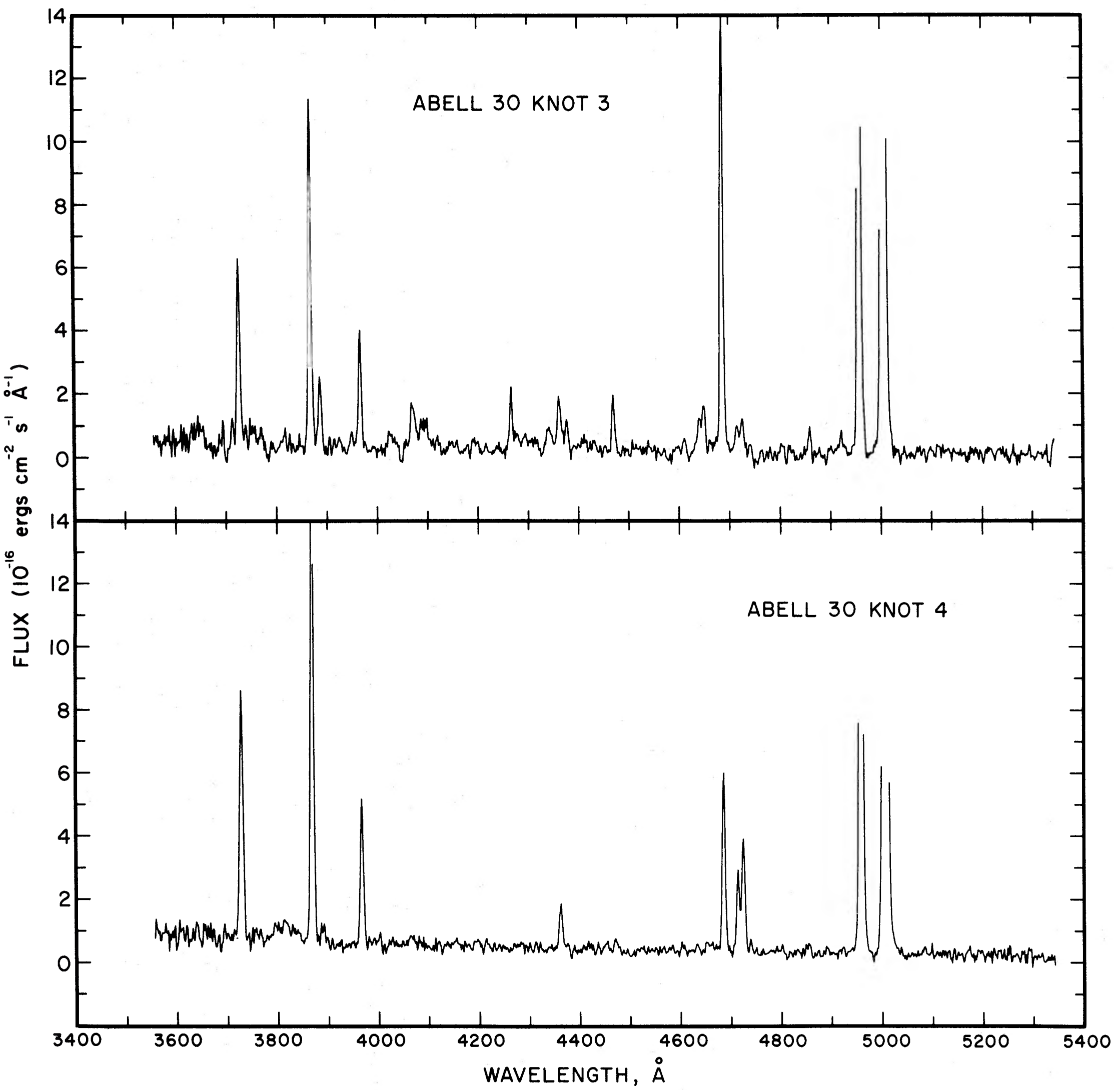

FIG. 3.—As for Fig. 1, but vertically expanded to show the weaker lines in Abell 30

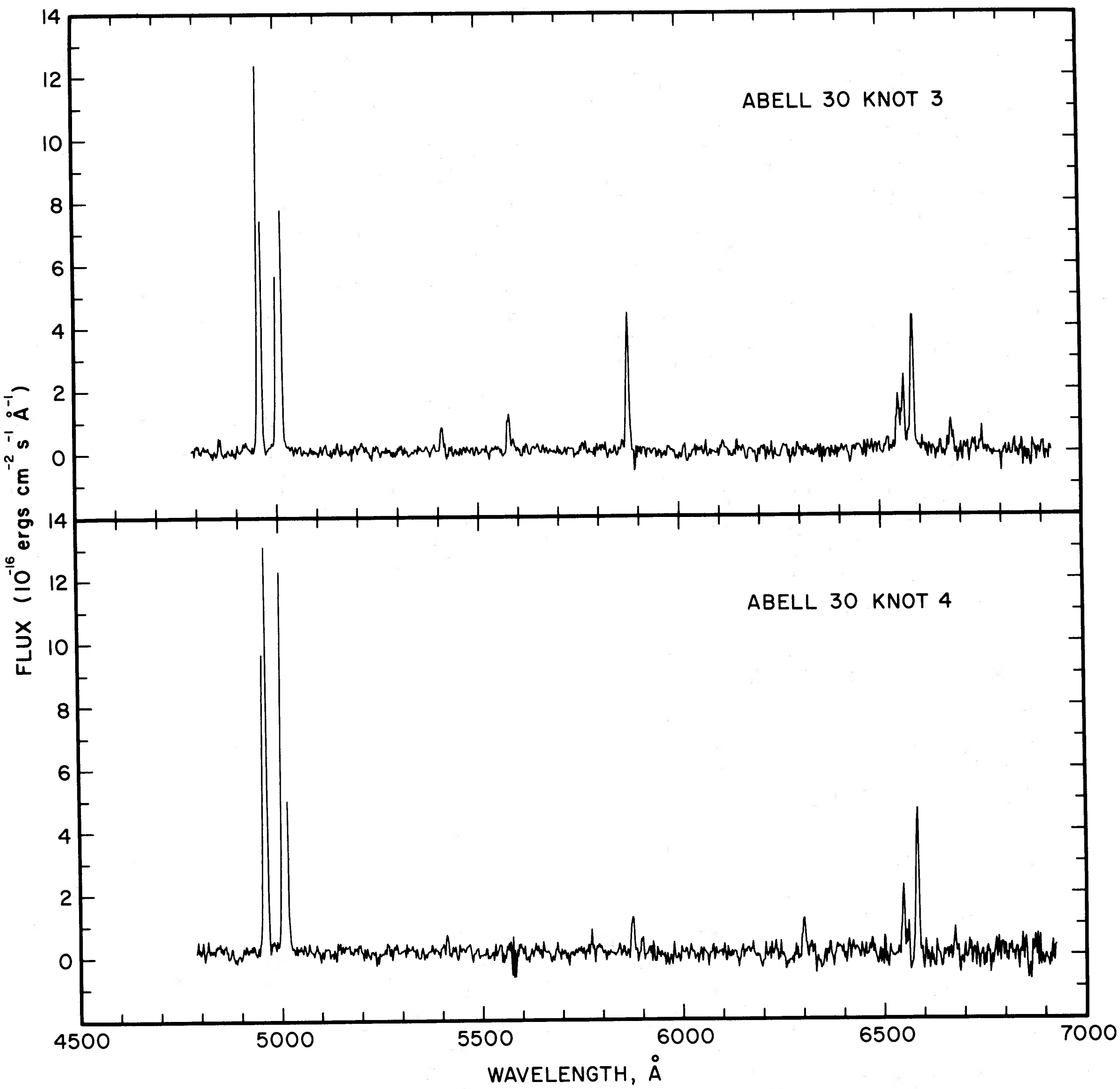

FIG. 4.—As for Fig. 2, but vertically expanded to show the weaker lines in Abell 30. The emission lines at 5577 Å and 6300 Å are residuals from incomplete sky subtraction due to variations in the strengths of these sky lines.

$I(\lambda 5007)$; the line ratios may be in error by 50% if the lines are weaker than 10% of $I(\lambda 5007)$. Unreliable measurements are marked with a colon; upper limits are preceded by "<". Because Abell 30 has brighter knots than Abell 78, the uncertainties are somewhat smaller than those given above.

III. PHYSICAL CONDITIONS: ELECTRON TEMPERATURE AND DENSITY

The usual procedures for deriving the physical conditions of the nebular plasma from diagnostic forbidden line ratios are of limited use in Abell 30 and Abell 78. While the electron temperature T_e can be calculated from the ratio of the [O III] lines $I(\lambda 4363)/I(\lambda 5007)$, the density-related line ratios using either [O II] $I(\lambda 3726)/I(\lambda 3729)$ or [S II] $I(\lambda 6717)/I(\lambda 6731)$ are of little value because the lines are so weak in these very high excitation nebulae.

An estimate of the electron density N_e can still be obtained if the distance to the nebula and the flux in Hβ or some other recombination line can be measured. For a homogeneous sphere of radius r, the observed extinction-corrected He II flux at $\lambda 4686$ is given by

$$F_{4686} = j_{4686} \frac{V_{\mathrm{neb}}}{d^2} , \quad (1)$$

where $4\pi j_{4686}$ is the emissivity for the $\lambda 4686$ transition, V_{neb} is the volume, and d is the distance to the nebula. The emissivity, which is a function of N_e and the

TABLE 1

LINE STRENGTHS RELATIVE TO $F(\lambda 5007) = 1.0$

	Abell 30 Knot 3		Abell 30 Knot 4		Abell 78	
Ion	*F*	*I*	*F*	*I*	*F*	*I*
λ3727 [O II]	0.062	0.088	0.081	0.115	0.064	0.074
λ3868 [Ne III]	0.111	0.150	0.132	0.179	0.160	0.182
λ3888 He I	0.021	0.028	...	...	...	...
λ3967 [Ne III]	0.036	0.047	0.041	0.054	0.033	0.037
λ4267 C II	0.018	0.022	<0.001	<0.001	<0.010	<0.011
λ4363 [O III]	0.021	0.025	0.014	0.016	0.014:	0.015:
λ4471 He I	0.014	0.016	...	...	...	...
λ4650 C III	0.020:	0.022:	...	...	...	...
λ4686 He II	0.151	0.163	0.050	0.054	0.121	0.125
λ4714 [Ne IV]	0.012:	0.013:	0.026	0.028	0.041	0.042
λ4725 [Ne IV]	0.015:	0.016:	0.032	0.034	0.059	0.061
λ4740 [Ar IV]	...	...	...	...	0.006:	0.006:
λ4861 Hβ	0.006	0.006	<0.002	<0.002	<0.004	<0.004
λ4959 [O III]	0.302	0.305	0.301	0.304	0.320	0.321
λ5411 He II	0.012:	0.011:	...	...	...	...
λ5876 He I	0.062	0.052	0.016	0.013	0.017	0.016
λ6548 [N II]	0.025:	0.018:	0.028	0.021	...	...
λ6563 Hα	0.032:	0.023:	...	...	...	...
λ6583 [N II]	0.077	0.056	0.066	0.048	0.022	0.019
λ6678 He I	0.012	0.009	0.010:	0.007:	...	...
log F_{5007}	−13.19		−13.14		−13.92	
c	0.44		0.44		0.185	

He^{++} density, varies only slightly with electron temperature. After rewriting, we have

$$F_{4686} = \frac{1}{3} N_e N_{\mathrm{He}^{++}} \alpha(4686, T_e) h\nu_{4686} \frac{r^3}{d^2}, \quad (2)$$

where $\alpha(4686, T_e)$ is the effective recombination coefficient. Further, we have

$$N_e = N_{\mathrm{H}^+} + N_{\mathrm{He}^+} + 2N_{\mathrm{He}^{++}} \quad (3)$$

or

$$N_{\mathrm{He}^{++}} = N_e \left(\frac{N_{\mathrm{H}^+}}{N_{\mathrm{He}^{++}}} + \frac{N_{\mathrm{He}^+}}{N_{\mathrm{He}^{++}}} + 2 \right)^{-1}. \quad (4)$$

To proceed further, we must already know the relative ionic concentrations of hydrogen and helium, although for the objects Abell 30 and Abell 78, we can make the initial assumptions that $N_{\mathrm{H}^+}/N_{\mathrm{He}^{++}} = 0$, $N_{\mathrm{He}^+}/N_{\mathrm{He}^{++}} = 1$, and $T_e \approx 15{,}000$ K. Then $N_{\mathrm{He}^{++}} = N_e/3$, and $\alpha(4686, T_e) \approx 2.5 \times 10^{-13}$ cm^3 s^{-1}. These parameters can then be iterated after determining the electron temperature and the actual ionic concentrations. From equations (2) and (4) we have

$$N_e^2(\mathrm{rms}) = \frac{F_{4686}[(N_{\mathrm{H}^+}/N_{\mathrm{He}^{++}}) + (N_{\mathrm{He}^+}/N_{\mathrm{He}^{++}}) + 2]}{\Gamma \alpha(4686, T_e) r''^3 d}, \quad (5)$$

where $\Gamma = 5 \times 10^{-10}$ for F_{4686} in ergs cm^{-2} s^{-1}, with d in parsecs and r in arcsec.

When N_e(rms) is derived from the hydrogen Balmer lines, it often differs from densities obtained from forbidden line ratios, usually being too small by factors as large as 4 (Torres-Peimbert and Peimbert 1977). This is generally attributed to the assumption of a homogeneous sphere when density fluctuations are actually present. Fortunately, the densities derived here are sufficiently low that even this large an uncertainty does not bear on the subsequent abundance analysis.

The derived densities and temperatures are included in Table 2. Masses of the observed regions are tabulated based on the derived N_e(rms) and the volume. Distances are those given by Cohen *et al.* (1977), 1400 pc for Abell 30 and 1700 pc for Abell 78. The densities in Table 2 are approximately 4–10 times larger than those derived by Abell (1966) and used by Cohen and Barlow (1974). Because Abell's densities are based on

TABLE 2

IONIC CONCENTRATIONS, $12 + \mathrm{LOG}\ [N_X/N_H]$

Parameter	Abell 30 Knot 3	Abell 30 Knot 4	Abell 78
T_e (K)	16,400	13,400	13,000
$\langle N_e \rangle$	400	200	100
Mass, $M_\odot$	0.0009	0.0005	0.00006
Ion:			
λ3727 O^+	7.97	8.84	8.42
λ3868 Ne^{++}	8.68	9.49	9.25
λ4267 C^{++}	11.63	<10.75:	<11.49:
λ4686 He^{++}	12.39	12.38	12.45
λ4725 Ne^{+3}	9.75	11.12	11.20
λ5007 O^{++}	9.13	9.86	9.62
λ5876 He^+	12.87	12.73	12.50
λ6583 N^+	7.80	8.36	7.72

the flux from the faint outer nebulae, it is not surprising that his values are smaller. When our values are plotted in Figures 5 and 7 of Cohen and Barlow (1974), the discrepancies attributed to these planetary nebulae are greatly reduced, because the infrared flux is now being related to the density in the correct emitting region. In fact, when the density is corrected by a factor of 2–4 for consistency with forbidden line values, both Abell 30 and Abell 78 fit the 10 μm flux versus density and the infrared color versus density relations very well.

Our densities appear to resolve the apparent departure from the relationships observed and predicted by Cohen and Barlow (1974). However, those authors assumed the dust is heated by trapped Lyα radiation. Because hydrogen is underabundant by more than a factor of 10, the Lyα production rate is down by a similar factor. But the overabundance of helium and the higher energy of the Lyα photons radiated during recombination by the singly and doubly ionized species of helium very nearly compensate for the inadequate heating from hydrogen Lyα.

IV. ABUNDANCES

a) Ionic Concentrations

When detailed information about the physical conditions in a nebula is known, the temperature fluctuation scheme (Peimbert and Torres-Peimbert 1977) is often used. We do not think our data warrant such an analysis, nor would the small differences in the results be significant compared with the extreme situations we are discussing. We therefore assume that no fluctuations are present ($t^2 = 0$) and note that our abundances will tend to be somewhat lower than a comparable analysis with $t^2 > 0$.

The ionic concentrations relative to hydrogen are calculated according to the usual relations. See, for example, Torres-Peimbert and Peimbert (1977), whose ionization correction scheme we adopt to account for unobserved stages of ionization. Note that our values relative to hydrogen are very uncertain due to the extremely weak or immeasurable strength of Hβ. Because this makes comparison with other objects (e.g., Orion, Sun, other planetary nebulae) inconvenient, we rectify this problem shortly (§ IV*b*).

The ionization correction scheme used relies on the coincidences of ionization potentials; however, the unusual composition of the knots and central star may introduce charge transfer effects and modifications to the ionizing spectrum which have not been considered.

Table 2 lists all the ionic concentrations for ions with measurable line strengths. To reduce possible systematic errors introduced by the weaker line measurements, the values are based on measurements of the strongest line from a given species (e.g., λ5876 of He I). Table 3 lists the calculated ionization correction factors (ICF) and the subsequent total elemental abundances relative to the hydrogen upper limit. As is often the case, the nitrogen ionization correction factor is quite large, and its elemental abundance should be considered uncertain.

The carbon abundances are derived from the λ4267 line and corrected for unseen stages of ionization following Torres-Peimbert and Peimbert (1977). The C^{+3} blend at λ4650 was detected in Abell 30 knot 3 and yields nearly the same ionic concentration as that obtained from the ionization correction method.

Carbon abundances derived from the λ4267 line are questionable because they are usually higher than those derived from the UV lines and vary from point to point within a nebula (Harrington, Lutz, and Seaton 1981; Barker 1982). Barker (1982) found the discrepancy in the Ring Nebula could be as high as a factor of 10 above the UV results, with the deviation increasing with decreasing distance from the central star. Torres-Peimbert and Peimbert (1977) argue that resonance fluorescence is not generally responsible for these differences in planetary nebulae. Grandi (1976) also concludes that the fluorescence process is not effective for the lower excitation conditions in the Orion Nebula.

Barker (1982) considers several possible sources for the discrepancy in the derived abundances in the Ring Nebula: charge transfer, dielectronic recombination, blending of the λ4267 line with an unidentified high-excitation line, and resonance fluorescence. He prefers the latter explanation for high-excitation regions but notes that carbon abundances inferred from the λ4267 line should be used with caution until the problem is better understood.

The derived carbon abundance in knot 3 of Abell 30 is probably too high for yet another reason. The predicted flux of the UV carbon lines will be approximately two orders of magnitude higher than the flux in the [O III] λ5007 line if we assume the derived abundances are accurate. It would then be difficult to maintain the high electron temperature (16,400 K) if

TABLE 3

ELEMENTAL ABUNDANCES, 12 + LOG [N_X/N_H]

	Abell 30 Knot 3		Abell 30 Knot 4		Abell 78	
Element	ICF	Abundance	ICF	Abundance	ICF	Abundance
He	1.00	12.99	1.00	12.89	1.00	12.78
O	1.33	9.32	1.44	10.06	1.88	9.89
N	22.1	9.14	16.8	9.59	31.8	9.19
Ne	1.42	8.83	1.58	9.69	2.00	9.52
C	1.83	11.89	1.54	<10.94:	1.84	<11.73:

the nebula is so effectively cooled through the carbon lines.

Lacking UV observations, the carbon abundances derived from the $\lambda 4267$ line will be used, but they should be considered uncertain and may be too high by as much as a factor of 10.

The neon line at $\lambda 4724$ is extremely strong in all the knots, approaching half the strength of F_{4686}. This implies an enormous quantity of Ne^{+3} if the computed ionic concentration reflects the true composition. However, $\lambda 4724$ is extremely temperature sensitive and is not considered a reliable diagnostic; it is usually advisable to ignore the results for this line (Kaler 1978).

b) Correction for Hydrogen Burning

We see from Table 3 that $N(\mathrm{He})/N(\mathrm{H})$ is typically 7 or more in Abell 30 and Abell 78. This represents an overabundance of 70 (usually $N(\mathrm{He})/N(\mathrm{H}) = 0.10$). When we consider that the Hβ line strength is an upper limit in two of the three cases, and that some column length through the more normal composition outer nebulosity is included in the observing aperture, the values for $N(\mathrm{He})/N(\mathrm{H})$ must be considered strict lower limits with nearly 100% hydrogen-to-helium processing.

Because the Hβ line strength is uncertain, the abundances in Table 3 are not especially useful for comparison with other nebulae. Also, elements other than helium appear artificially overabundant if significant hydrogen depletion has occurred. For discussion purposes, we would like to know the abundances of the elements relative to the initial hydrogen and helium composition. We make the assumptions that (1) these objects initially consisted of a normal ratio of $N(\mathrm{He})/N(\mathrm{H}) = 0.10$, and (2) the current situation has arisen because of total nuclear processing such that every four hydrogen nuclei result in a single helium nucleus. We denote the initial hydrogen and helium abundances by N_{H}^0 and N_{He}^0. Then we have

$$N_{\mathrm{He}} = N_{\mathrm{He}}^0 + \frac{N_{\mathrm{H}}^0}{4} \tag{6}$$

or

$$N_{\mathrm{He}} = 0.35 N_{\mathrm{H}}^0 \; . \tag{7}$$

From equation (7) and the values in Table 3 for the observed abundances relative to hydrogen, we compute the current abundance of each element relative to the initial hydrogen abundance. These values are given in Table 4 in the usual logarithmic notation. In subsequent columns, average values for these elements are given as found in other planetary nebulae (PN), Orion, and the Sun.

c) Variations in Abell 30

The abundances derived from the forbidden lines in Abell 30 knot 3 are approximately a factor of 6 below those found in knot 4. The carbon abundance, on the other hand, is considerably higher. To some extent this can be attributed to an overestimate of the electron temperature in knot 3. If T_e is reduced to 13,400 K, as in knot 4, the relative abundances of O, Ne, and N are increased by a factor of 2. To fully compensate for the factor of 6, T_e must be reduced to about 9000 K. This temperature reduction corresponds to a factor of 5 measurement error in the temperature-sensitive line of [O III] $\lambda 4363$, whereas reducing the temperature to that of knot 4 only implies an error of 30%. Furthermore, the high carbon abundance would remain. We estimate that if the temperature were, in fact, only 9000 K, we probably would have been just able to detect the $\lambda 4363$ line, but not measure its strength reliably.

Another indication of a high temperature for knot 3 is the presence of a weak blend at 4070 Å. If we identify this feature with the [S II] doublet at $\lambda\lambda 4068$, 4076, then the ratio of $I(\lambda 4068) + I(\lambda 4076)/I(\lambda 6717) + I(\lambda 6731)$ can also be used to derive the electron temperature. Since the red [S II] lines are too weak to measure, this ratio must be large, suggesting a high temperature. The relatively poor red sensitivity of the instrument introduces considerable uncertainty into this ratio.

If an alternative heating mechanism such as shock excitation is present, the [O III] temperature ratio cannot be interpreted with the usual photoionization assumptions because of steep temperature gradients behind the shock front (Cox 1972). In fact, a shock velocity of less than 50 km s^{-1} is sufficient to excite the $\lambda 4363$ and $\lambda 5007$ lines to the observed ratio (Raymond 1979). A possible source for the mechanical energy of the shock is the stellar wind (§ V*b*) originating at the central star. If the mass loss rate from the star is on the order of 10^{-7}–10^{-6} $M_\odot$ per year, the mechanical power will be comparable to the luminosity of the star. Confining

TABLE 4

ELEMENTAL LOGARITHMIC ABUNDANCES RELATIVE TO INITIAL HYDROGEN

Element	Abell 30 Knot 3	Abell 30 Knot 4	Abell 78	PN	Orion	Solar
He/H[a]	9.9	>7.8	>6.0	0.11	0.10	0.06:
O	7.87	8.71	8.66	8.9	8.52	8.84
N	7.69	8.24	7.96	8.3	7.57	7.94
Ne	7.38	8.34	8.29	8.3	7.66	7.57
C	10.44	<9.60:	<10.5:	9.5	8.55:	8.62

NOTE.—PN: from Peimbert 1978; Orion: from Peimbert and Torres-Peimbert 1977; solar: from Ross and Aller 1976.

[a] Ratio by number.

shock excitation to one knot, though, presents a symmetry problem.

Variations in the extinction correction caused by dust localized in the knots may have some effect on the derived abundances. If, in fact, no dust were present toward knot 3, the temperature could be reduced slightly from the 13,400 K in knot 4 to about 12,700 K—but not to the 9000 K required to match the abundances in knot 4. Alternatively, if the extinction in knot 4 were greatly increased, the temperature could be raised to the point where the abundances drop to the levels seen in knot 3.

Although this is a plausible, albeit ad hoc, mechanism to equalize the abundances in the two knots, we prefer to accept the values from knot 4 because (1) they agree well with the accepted composition of other objects, and (2) the spectrum of knot 3 is peculiar in other respects.

Several lines in knot 3 are not seen or seen only weakly in other planetary nebulae. For example, the carbon lines, $\lambda 4267$ and $\lambda 4650$, are extremely strong, leading to the high derived carbon abundance. Also, the permitted N III $\lambda 4379$ line is rarely seen, yet here it is nearly half the strength of $\lambda 4363$. And in contrast to knot 4 and Abell 78, Hβ is measurable. Furthermore, the ionization levels in knot 3 appear significantly lower than those in either knot 4 or Abell 78, as evidenced by the greater strength of the He I lines and the relative weakness of the Ne IV line.

We tentatively conclude that knot 3 differs from knot 4 in its chemical composition. We suggest that if this is due to compositional segregation in the progenitor, knot 1, which is symmetrically paired across the central star with knot 3, may also have low abundances.

V. DISCUSSION

a) *Helium Nebulae*

Enhancement of the helium abundance in planetary nebulae is a common phenomenon. Usually the composition is limited to $N_{\rm He}/N_{\rm H} < 0.3$, which corresponds to enrichment by less than a factor of 3. Observations of planetary nebulae are in good agreement with evolutionary models of planetary nebula progenitors in which a convective zone in the hydrogen envelope "dredges up" helium and nitrogen from the nuclear-processed material in the star's underlying layers (Kaler, Iben, and Becker 1978).

The processes causing the extreme conditions in Abell 30 and Abell 78 are different from those described above. Here we are not seeing enriched material (i.e., a normal composition mixed with processed material). Rather, we are seeing directly the end results of nuclear processing in a hydrogen-burning shell, with conversion to helium approaching 100% completion.

Despite the absence of hydrogen, the relative abundances of the elements O, N, Ne, and C are all in good agreement with the compositions in more normal planetary nebulae. The notable exception is Abell 30 in knot 3, where O, N, and Ne are all deficient by a factor of 3–6, and C is overabundant by a factor of 8. It may be that the underlying helium-burning zones have been dredged up, thereby enhancing the carbon abundance in the same way that nitrogen and helium are enhanced in normal planetary nebulae. Nevertheless, the different compositions in the knots of Abell 30 appear to be real and argue for chemical segregation prior to the ejection of the helium layer. This process may be related to the mechanism for ejection of four knots symmetrically oriented about the central star (Jacoby 1979).

b) *Multiple-Shell Planetary Nebulae*

Abell 30 and Abell 78 are members of the small group of planetary nebulae which have multiple shells. About 25 such nebulae are known (Kaler 1974); of these, a handful have three shells. All multiple-shell planetary nebulae other than Abell 30 and Abell 78 exhibit hydrogen line emission in all shells, although a detailed study of abundance variations from shell to shell has not yet been done and would be of considerable interest.

Having undergone two nebular ejections, the central stars of Abell 30 and Abell 78 may now have carbon-rich atmospheres. The spectra taken by Cohen *et al.* (1977) are dominated by strong, broad (~ 700 km s^{-1}) C IV lines in emission and weak helium lines in absorption. Furthermore, the sum of the estimated masses ($\sim 10^{-3}\ M_\odot$) for the helium knots is comparable to the helium-atmosphere masses (10^{-4}–$10^{-2}\ M_\odot$, D'Antona and Mazzitelli 1979) expected for hot subdwarfs. The agreement suggests that much of the helium envelope may have been blown off during the ejection, although the envelope mass is somewhat dependent on the progenitor core mass (Paczyński 1975).

The central stars may in fact be in the process of further expelling material. Greenstein and Minskowski (1964) and Cohen *et al.* (1977) note the presence of broad lines corresponding to motions on the order of 1000 km s^{-1}. Heap (1979) observed Abell 78 with the *International Ultraviolet Explorer* (*IUE*) and found P Cygni–type profiles in the lines of N V $\lambda 1240$, O V $\lambda 1370$, and C IV $\lambda 1550$. The estimated terminal velocity for these lines is 3400 km s^{-1}, indicating a large luminosity-to-mass ratio. Similar P Cygni characteristics were also found in Abell 30 by Greenstein (1980).

c) *Abundances and Stellar Interiors*

The stellar structure prior to planetary nebula ejection is generally considered to consist of (1) a carbon-oxygen core, (2) a helium shell which is the product of CNO burning, and (3) a hydrogen-rich envelope. During nebular ejection the outer hydrogen-rich envelope is removed down to the mean molecular weigh discontinuity of the helium shell.

During equilibrium CNO hydrogen-shell burning, hydrogen is depleted to within a few percent of totality, and essentially all the carbon and oxygen are converted to nitrogen because of the long lifetime of N^{14} against proton capture. We see from Table 4 that the hydrogen is depleted to less than 20% (the observational upper limit) in Abell 78 but could be less than 3% in Abell 30 knot 3.

The nitrogen abundance is more difficult to measure accurately because of the large ionization correction factor and the relatively low strength of the emission at $\lambda 6584$. The trend in the ratios of nitrogen to oxygen abundance seen in Table 4 is one of general agreement with other planetary nebulae, which exhibit a factor of 2–4 enrichment of nitrogen relative to Orion. The exception is Abell 30 knot 3 which seems to be either nitrogen overabundant or oxygen depleted.

The carbon abundance in hydrogen-depleted zones is expected to be enhanced due to convective mixing with the carbon-oxygen core. This mixing also replenishes those species depleted during the CNO conversion to nitrogen. The carbon fraction should be (Iben and Truran 1978)

$$X_{\rm C} = 0.25(M_c - 0.16)\,, \tag{8}$$

where M_c is the core mass, usually in the neighborhood of 0.6 $M_\odot$. The predicted value of $X_{\rm C}$ is thus 0.11, and the observed values for Abell 30 knots 3 and 4 and Abell 78 are 0.08, <0.01, and <0.09, respectively. We again stress that the carbon abundances are uncertain, but we find some agreement with the values from the models.

d) *Frequency of Helium-Shell Planetary Nebulae*

The frequency of occurrence of planetary nebulae in this helium-shell class appears to be small. This can be attributed to some unusual event in their history, to a limited number of planetary nebula progenitors which produce helium shells, to the absence of suitable surveys for the detection of such nebulae, or to a short lifetime of the helium shells.

There is some possibility that the evolution of these objects has been affected by companion stars (Cudworth 1974; Jacoby 1979). However, the separations (0.05–0.1 pc) of the visible components are generally considered too large for interaction, although there have been no searches for close unseen companions.

Another possibility is that helium shells are ejected only by progenitor stars that lie within a certain range of mass, angular momentum, or chemical composition.

There is reason to believe that the helium shells will dissipate more rapidly than normal planetary nebula shells because their masses are considerably smaller. Detectability is possible until the flux received from the helium shell falls below some critical limit which is determined by the detector and the sky brightness. This critical flux limit is the same both for helium shells and shells of normal composition. For detections made in the [O III] line at $\lambda 5007$,

$$S_{5007} \propto \frac{N_e N_{\rm O^{++}} V}{A}\,, \tag{9}$$

where V and A are the volume and surface area of the nebula. We obtain N_e from equation (3), where

$$N_{\rm H^+} = \frac{M_{\rm H}}{m_{\rm H} V}\,, \tag{10}$$

$$N_{\rm He^+} \equiv f N_{\rm He} = f\,\frac{M_{\rm He}}{4m_{\rm H} V}\,, \tag{11}$$

$$N_{\rm He^{++}} = (1-f)N_{\rm He} = (1-f)\frac{M_{\rm He}}{4m_{\rm H} V}\,. \tag{12}$$

By combining equations (3) and (10)–(12), we have

$$N_e = \frac{4M_{\rm H^+} f M_{\rm He} + 2(1-f)M_{\rm He}}{4m_{\rm H} V}\,. \tag{13}$$

If the fraction of oxygen atoms relative to the initial composition does not change (no oxygen is synthesized), and excitation levels remain the same, then

$$N_{\rm O^{++}} \approx g\left(\frac{4M_{\rm H} + 4M_{\rm He}}{4m_{\rm H} V}\right). \tag{14}$$

We assume the following parameters for the ejected helium shells: $f \approx 0.5$, $M_{\rm H} = 0$, $M_{\rm He} \approx 0.001\ M_\odot$. For shells of normal composition, $f \approx 0.8$, $M_{\rm H} \approx 0.2\ M_\odot$, and $M_{\rm He} \approx 0.1\ M_\odot$. We further assume that the oxygen abundance parameter g is the same in both cases.

From equations (9)–(14), we find that

$$\frac{r(\text{helium shell})}{r(\text{normal shell})} \approx 0.09 \tag{15}$$

at the critical surface brightness limit. If both helium and normal-composition shells expand at the same rate, the relative lifetimes of the two types of shells are directly proportional to the radius ratio. If the lifetime of a normal planetary nebula shell is 25,000 yr, then the helium-shell lifetime is approximately 2200 yr. During this detection period, the diameter of the shells will increase by 0.09 pc if the expansion velocity is 20 km s^{-1}.

Because Abell 30 and Abell 78 are approximately the same size (0.8 and 0.84 pc, respectively), we conclude that the helium-zone phenomenon occurs late in the evolution of planetary nebulae. Of the 49 Abell planetary nebulae surveyed by Jacoby (1979), 31 have diameters exceeding 0.5 pc (Abell 1966). If we propose that all planetary nebulae pass through the helium-ejection phase upon reaching 0.8 pc and then are visible for 2200 years (until their diameters extend to 0.89 pc), we would expect some fraction of these 31 nebulae to have helium shells.

Estimating the fraction is complicated by the uncertainty in the distances and hence, the diameters of these nebulae. For a normal distribution about the expected diameter, we find that for diameter uncertainties of 10%, 30%, and 50%, we expect 4.0, 3.2, and 2.5 planetary nebulae to have diameters within the helium-shell limits. In fact, we find two: Abell 30 and Abell 78. Clearly, the sample is too sparse to allow reliable conclusions, but the data suggest that there may be many helium-zone planetary nebulae, and that, perhaps, two-thirds of all planetary nebulae pass through a helium-ejection phase.

We would then expect that a large fraction of white dwarfs should have either helium or carbon atmospheres. But the interpretation of the subsequent evolutionary stages of the descendants of Abell 30-type central stars is complicated by processes such as accretion and diffusion (Liebert 1980). We simply note that helium white dwarfs are not unusual and several C_2 white dwarfs are also known.

If two-thirds of all planetary nebulae eject helium shells, the average interstellar helium-enrichment mass per planetary nebula is $\frac{2}{3}10^{-3}\ M_{\odot}$ from this process. The helium enrichment per planetary nebula from the helium excess (20% by number) in the hydrogen shell will be approximately 10 times this amount. Depending on the fraction of planetary nebulae ejecting helium shells, a moderate percentage of the Galaxy's helium enrichment may be attributed to this process.

VI. CONCLUSIONS

Several classes of stars and nebulae which are late stages of stellar evolution exhibit large helium overabundances: supernova remnants, white dwarfs, Wolf-Rayet stars, and R CrB stars. Abundance analyses for these objects are model dependent or complicated by mixing with the interstellar medium. The nebulae discussed here, Abell 30 and Abell 78, provide a straightforward way to investigate the composition of the end products of a hydrogen-burning shell.

The shells recently ejected in Abell 30 and Abell 78 are extremely hydrogen deficient, but after accounting for complete conversion of hydrogen to helium, the relative abundances of O, N, and Ne are not very different from the values typically encountered in normal planetary nebulae. Some enhancement of the carbon abundance, however, is suggested.

Despite the unusual nature of the helium shells in Abell 30 and Abell 78, the phenomenon appears to be a common, though short-lived, phase in the evolution of older planetary nebulae.

We wish to thank Robin Ciardullo for reducing the data taken at Lick Observatory, and Dr. P. Harrington for useful discussions concerning the carbon abundances.

REFERENCES

Abell, G. O. 1966, *Ap. J.*, **144**, 259.
Barker, T. 1982, *Ap. J.*, **253**, 167.
Cohen, M., and Barlow, M. J. 1974, *Ap. J.*, **213**, 737.
Cohen, M., Hudson, H., O'Dell, S., and Stein, W. A. 1977, *M.N.R.A.S.*, **181**, 233.
Cox, D. P. 1972, *Ap. J.*, **178**, 143.
Cudworth, K. 1974, *A.J.*, **79**, 1384.
D'Antona, F., and Mazzitelli, I. 1979, *Astr. Ap.*, **74**, 161.
Grandi, S. A. 1976, *Ap. J.*, **206**, 658.
Greenstein, J. 1980, *Ap. J.*, **245**, 124.
Greenstein, J., and Minkowski, R. 1964, *Ap. J.*, **140**, 1601.
Harrington, J. P., Lutz, J. H., and Seaton, M. J. 1981, *M.N.R.A.S.*, **195**, 21p.
Hazard, C., Terlevich, R., Morton, D. C., Sargent, W. L. W., and Ferland, G. 1980, *Nature*, **285**, 463.
Heap, S. R. 1979, in *IAU Symposium 83, Mass Loss and Evolution of O-Type Stars*, ed. P. S. Conti and C. W. H. de Loore (Dordrecht: Reidel), p. 99.
Iben, I., and Truran, J. W. 1978, *Ap. J.*, **220**, 980.
Jacoby, G. H. 1979, *Pub. A.S.P.*, **91**, 754.
Kaler, J. B. 1974, *A.J.*, **79**, 574.
———. 1978, *Ap. J.*, **225**, 527.
———. 1981, *Ap. J. (Letters)*, **250**, L31.
Kaler, J. B., Iben, I., and Becker, S. A. 1978, *Ap. J. (Letters)*, **224**, L63.
Liebert, J. 1980, *Ann. Rev. Astr. Ap.*, **18**, 363.
Paczyński, B. 1975, *Ap. J.*, **202**, 558.
Peimbert, M. 1978, in *IAU Symposium 76, Planetary Nebulae*, ed. Y. Terzian (Dordrecht: Reidel), p. 215.
Peimbert, M., and Torres-Peimbert, S. 1977, *M.N.R.A.S.*, **179**, 217.
Raymond, J. C. 1979, *Ap. J. Suppl.*, **39**, 1.
Ross, J. E., and Aller, L. H. 1976, *Science*, **191**, 1223.
Torres-Peimbert, S., and Peimbert, M. 1977, *Rev. Mexicana Astr. Ap.*, **2**, 181.
Whitford, A. E. 1958, *A.J.*, **63**, 201.

HOLLAND C. FORD: Space Telescope Science Institute, Homewood Campus, Baltimore, MD 21218

GEORGE H. JACOBY: Kitt Peak National Observatory, P.O. Box 26732, Tucson, AZ 85716